Alkali treatment of hemp fibres for the production of aligned hemp fibre mats for composite reinforcement

Sunny, Tom*; Pickering, Kim L; Lim, Shen Hin

School of Engineering, The University of Waikato, Gate 8, Hillcrest Road, Hamilton, 3240, New Zealand

*Correspondence to: Email: tomsunny54@gmail.com

Abstract

The main objective of this study was to produce aligned hemp fibre mats from high strength hemp fibres using dynamic sheet forming (DSF). Alkali treatment of hemp fibre was carried out at ambient and high temperature to separate fibres. Single fibre tensile testing was used to assess the tensile properties of the fibres. It was found that the highest tensile properties were exhibited by high temperature treated fibre, whereas the tensile properties exhibited by ambient temperature treated fibre were lower than for untreated fibre. It was also found that fibre granulated after high temperature treatment, was better separated than that granulated before high temperature treatment. This well-separated fibre could successfully be formed into mats using DSF. The orientation of the formed mat was analysed using ImageJ (NIH, USA) software by which the potential of DSF to produce aligned hemp fibre mat was supported. The mechanical performance of composite reinforced by these aligned hemp fibre mats were assessed.

Keywords: *Dynamic sheet forming (DSF); Alkali treatment; Aligned fibre mats; Hemp fibre*

1. Introduction

A major area of recent technological development has been that of natural plant fibre composites (NPFCs). Generally, NPFCs consist of plant fibres as reinforcement in a polymer matrix. Natural plant fibres (NPFs) have undergone increased industrial uptake because of their favourable characteristics such as lower density, higher specific strength and stiffness, lower cost, and with lower associated hazards during manufacture (Pickering 2008, Kabir, Wang et al. 2012, Kabir, Wang et al. 2013, Pickering, Efendy et al. 2015). Hemp fibres are attractive reinforcements for NPFCs as they exhibit high tensile strength ranging between 550-1110 MPa (Beckermann and Pickering 2008, Pickering, Efendy et al. 2015). Hemp fibres are also more environmentally friendly than most fibres since they can be grown without pesticides and herbicides.

The main reasons that limit NPFCs in industry are moisture absorption, lower strength and greater variability of properties compared to synthetic fibre composites (Pickering, Efendy et al. 2015). Previous research has shown that chemical treatments of reinforcing fibres can help to overcome these limitations (Mwaikambo and Ansell 2002, Li, Tabil et al. 2007, John and Anandjiwala 2008, Kabir, Wang et al. 2012, Pickering, Efendy et al. 2015). Among the different chemical treatments, alkali treatment with sodium hydroxide (NaOH) is the most widely used. This treatment removes fibre constituents such as pectin, hemicellulose, lignin and waxes from NPFs bringing about fibre separation and can enhance fibre properties (Beckermann and Pickering 2008, Islam, Pickering et al. 2011, Pickering, Efendy et al. 2015). Modest treatments have been seen to bring about increased cellulose crystallinity, which is considered to be due to the removal of the aforementioned materials, whereas harsher treatments have been shown to convert crystalline cellulose to amorphous cellulose and possibly resulted in chain scission (Sawpan, Pickering et al. 2011, Kabir, Wang et al. 2012). These alkali treatments have been carried out by different researchers with varying process parameters including at ambient temperatures (AT) as well as at high temperatures (HT) (Mwaikambo and Ansell 2002, Beckermann and Pickering 2008, Islam, Pickering et al. 2010, Islam, Pickering et al. 2011, Sawpan, Pickering et al. 2011, Kabir, Wang et al. 2012, Kabir, Wang et al. 2013, Efendy and Pickering 2014). Ambient temperature treatments have many advantages such as simplicity, low cost and they can be easily carried out in large volumes compared to HT treatment. However, there is limited information available on the effect of alkali treatment temperature (high temperature versus ambient temperature) on the tensile properties of individual hemp fibres. Also, where the tensile properties are given, these values are based on variable testing regimes including: fibre bundles as opposed to single fibres and unspecified gauge lengths (Beckermann 2007). Therefore, direct comparison is needed between high temperature and ambient temperature treatment to inform which is best.

To encourage uptake of NPFCs, convenient forms of NPFs that could be used as alternatives to synthetic fibre mats in standard moulding operations would be helpful. Dynamic sheet forming (DSF) is a method that can be used to produce preferentially aligned short NPF mats (Sunny, Pickering et al. 2017). Previous studies have demonstrated that these mats can be incorporated into polymer matrices to produce composites, which exhibited higher tensile strength as well as Young's modulus compared to randomly oriented fibre mats composites (Pickering and Efendy 2016, Pickering and Le 2016, Sunny, Pickering et al. 2017). Prior to DSF, good fibre separation is

needed. Alkali treated hemp and harakeke fibres have been reported as used for the production of DSF mats, (Le and Pickering 2015, Pickering, Efendy et al. 2015, Ghazali and Efendy 2016) but the tensile strengths of these treated fibres were reduced compared to raw fibre due to the weakening of structural components (Islam 2008, Ghazali and Efendy 2016, Le 2016, Pickering and Efendy 2016). Therefore, further research is needed to develop processing parameters to improve fibre separation without reduction in tensile properties of fibres prior to DSF. In the current research, the alkali treatments used are modifications of selected alkali treatments from the literature that report improved tensile strength for NPFs (Beckermann and Pickering 2008, Oushabi, Sair et al. 2017). The data obtained for the tensile strengths of the hemp fibres were statistically analysed using Weibull statistics.

2. Experimental

2.1 Materials

Industrial hemp fibre was obtained from Moffett Orchards Ltd., New Zealand. The bast fibres were hand separated from the stalks. The chemicals used for the experiments were sodium hydroxide (NaOH) and sodium sulphite (Na_2SO_3) supplied by Sigma Aldrich. Polypropylene (PP) random copolymer SKRX3600 supplied by Clariant (New Zealand) Limited, with a melt index of 18 g/10min and a density of 0.9 g/cm^3, was used as the matrix. The coupling agent used was A-C 950P maleic anhydride polypropylene (MAPP) supplied by Honeywell International Inc., USA

2.2 Methods

2.2.1 Alkali treatment

High temperature (HT) and ambient temperature (AT) alkali fibre treatments were carried out on pre-dried hand separated hemp fibres. For ambient temperature treatment, fibres were granulated using an 8 mm mesh in a laboratory scale Castin granulator and then immersed in 5wt% sodium hydroxide (NaOH) solution in a glass beaker as shown in Fig. 1a, for one (AT/one hour) or two hours (AT/ two hours) with a fibre to solution ratio of 1:8. The temperature inside and outside the beaker was measured using a thermometer. The measured room temperature was between 20.5 °C and 22 °C, whereas the temperature inside the beaker ranged from 30.5 °C at the start of the

treatment to 24 °C at the end of the treatment. For high temperature treatment, fibre and a solution of 5wt% NaOH and 2wt% Na_2SO_3 with a fibre to solution ratio of 1:8 were placed in stainless steel canisters (SSCs) Fig. 1b. These canisters were then positioned inside a laboratory scale pulp digester controlled by a proportional-integral-derivative (PID) system as displayed in Fig. 1b, which was set to operate with a time-temperature profile as shown in Fig. 2. Granulation was either conducted before or after treatment. The fibres were washed after the treatments for about 15 minutes in clean water, before being dried in an oven at 80 °C for 48 h.

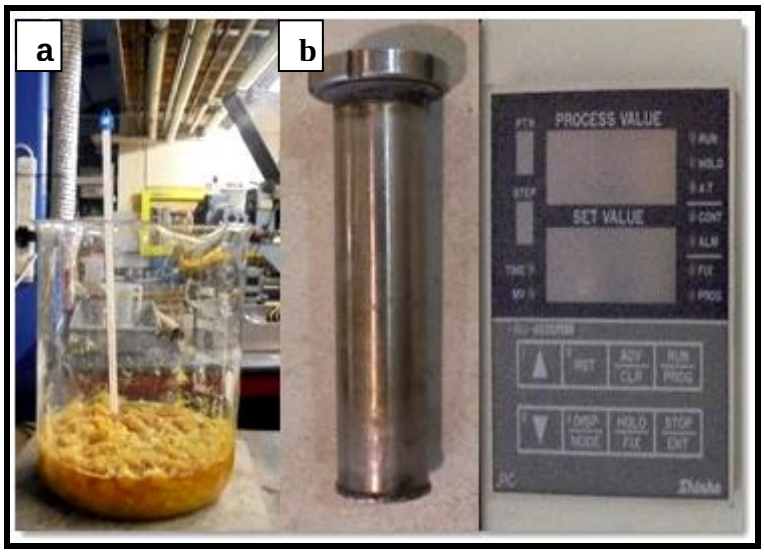

Fig. 1. (a) Set up used for the AT treatment (b) SSC and PID system used for the HT treatment.

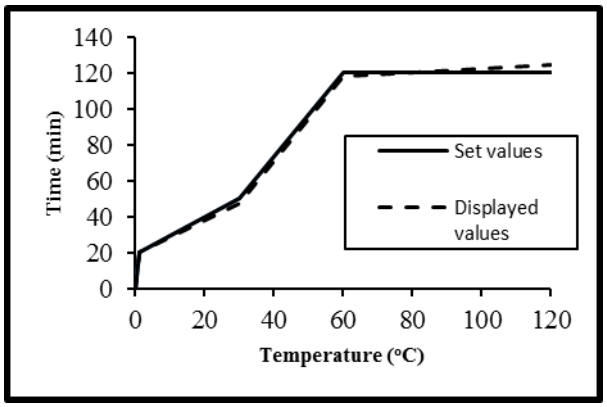

Fig. 2. Time-temperature profile used for the HT treatment.

2.2.2 Single fibre tensile testing

The ASTM D 3379-75: Standard Test Method for Tensile Strength and Young's Modulus for High-Modulus Single-Filament Materials (ASTM 1986) was followed to determine the tensile strength and Young's modulus of untreated (UT), AT/one hour treated, granulated before HT treated and granulated after HT treated hemp fibres. The untreated fibres were soaked in water for

around 10 days to remove dirt from the fibre surface. Two-millimetre thick cardboard was used for mounting tabs with a gauge length of two millimetres as schematically represented in Fig. 3. Selected single fibres were adhered to the mounting tabs by the application of polyvinyl acetate (PVA) glue.

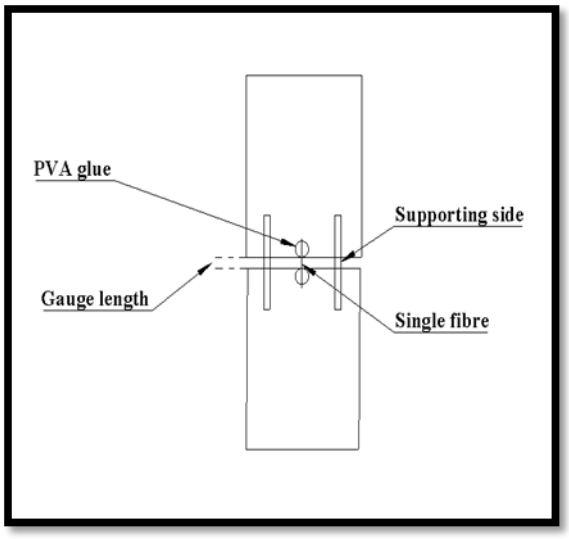

Fig. 3. Schematic representation of a mounting tab used for tensile testing of single fibres.

For the measurement of single fibre diameter, optical images were captured of single fibres as shown in Fig. 4, by means of an Olympus BX60F5 optical microscope fitted with a Nikon camera. The diameter was measured at five different points along each fibre (as hemp fibres have variable diameters across their length) and average values were used for the calculations.

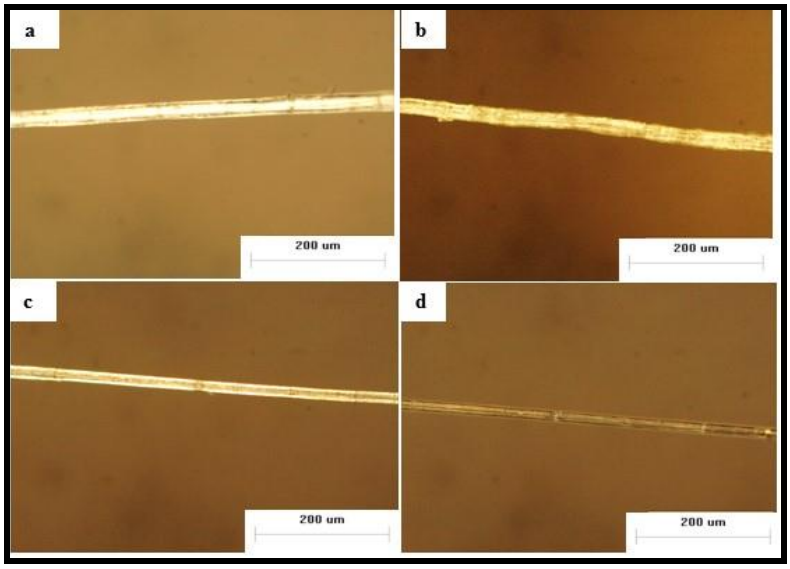

Fig. 4. Single hemp fibre as observed under optical microscope: (a) UT, (b) AT/one hour, (c) granulated before HT and (d) granulated after HT treated hemp fibres.

The single fibres were then tensile tested using an Instron-4204 universal testing machine after burning off the supporting sides using a hot wire cutter. The test was carried out at a rate of 0.5 mm/min with a 10 N-load cell. Thirty samples were tested for each treatment and system compliance was determined experimentally to obtain Young's moduli according to the procedure described in ASTM D 3379-75. For this, mounting tabs with gauge lengths of 5, 10 and 15 mm were also prepared.

The Weibull distribution is commonly used to analyse the strength variation for natural fibres (Biagiotti, Puglia et al. 2004, Pickering, Beckermann et al. 2007, Zafeiropoulos and Baillie 2007, Efendy and Pickering 2014). Here, the rearranged two-parameter Weibull cumulative distribution expression (Biagiotti, Puglia et al. 2004, Pickering, Beckermann et al. 2007), as shown below was used to analyse data obtained for different single fibre testing statistically.

$$\ln\ln (1/(1-P_f)) = w\ln\sigma - w\ln\sigma_o + \ln L \quad (1)$$

where w is the Weibull modulus (shape parameter) and σ_0 characteristic strength (scale parameter). These parameters are important as they describe the variability of the fibre failure strength (Zafeiropoulos and Baillie 2007). A Weibull plot of $\ln\ln (1/(1-P_f))$ versus $\ln\sigma$ provides a straight line with gradient w and intercept σ_o at $\ln\ln (1/(1-P_f)) = 0$.

2.2.3 Scanning electron microscopy (SEM) of hemp fibre surfaces

A Hitachi S-4100 SEM was used to obtain micrographs of fibres. Carbon tapes were employed to mount the samples on aluminium stubs and were then sputter coated with platinum to make them conductive.

2.2.4 Wide angle X-ray diffraction (WAXD)

To assess fibre crystallinity, a Philips X'Pert diffractometer fitted with a ceramic X-ray diffraction tube was used. For the measurements, the fibres were chopped and pressed into a disk using a cylindrical steel mould. The scanning range was between 5° and 45° by employing CuKα radiation (λ=1.54 nm) with a voltage and current of 45 mV and 40 mA respectively. Crystallinity index (I_c) of the fibres was calculated using the Segal method (Segal, Creely et al. 1959):

$$I_C = (I_{22.7} - I_{18.3}/I_{22.7}) \text{ X } 100 \quad (2)$$

where I_{200} is the maximum intensity of the (200) lattice diffraction peak at a 2θ angle of between 22° and 23°, and I_{am} is the minimum intensity of diffraction at an angle 2θ between 18° and 19° representing amorphous materials (Pickering, Beckermann et al. 2007, French 2014).

2.2.5 Fourier transform infrared spectroscopy (FTIR)

An FTIR Digilab FTS-40 was used to obtain infrared spectra of untreated, AT/one hour treated and granulated after HT treated hemp fibres. Hemp fibre samples were ground to fine powder using a Retsch MM400 ball mill. The ground powder for each sample was then mixed and compressed with KBr (potassium bromide) using a hydraulic press by applying 8 tonnes/cm^2 pressure to prepare corresponding sample disc for FTIR analysis.

2.2.6 Thermal analysis

Thermal gravimetric analysis (TGA) of untreated, AT/one hour treated and granulated after HT treated hemp fibres was carried out using a PerkinElmer simultaneous thermal analyser STA 800. Data were obtained at a rate of 10 °C/min with a heating range of 40 °C to 500 °C and a static airflow at 20 ml/min.

2.2.7 Fibre mat assessment

The OrientationJ plugin of ImageJ was used to assess the orientation of fibres in fibre mats. Availability and ease of use make ImageJ attractive (Abràmoff, Magalhães et al. 2004, Schneider, Rasband et al. 2012). The principles behind this analysis tool are available in the literature (Rezakhaniha, Agianniotis et al. 2012, Gesellchen, Bernassau et al. 2014, Shah, Vollrath et al. 2015, Püspöki, Storath et al. 2016, Sunny, Pickering et al. 2018). OrientationJ can provide a fibre orientation distribution profile based on the orientation of fibres within a mat analysed. The peak of the profile indicates the predominant orientation of fibres within the mat.

Additionally, with the calculation of majority of the orientation of fibres in an image, this program also calculates a 'coherency factor' to that orientation (Lewis 2016). This factor is calculated based on the amount of pixels that are in line in a particular direction and is bounded between 0 and 1; with 0 and 1 indicating isotropic and anisotropic orientations, respectively (Palmieri, Lucchetti et al. 2015). Twenty-five images, each of aligned and random mats were used for the analysis. All

the macroscopic images (Fig. 5 a and 5b) were taken using a Wild M3B stereomicroscope attached with Nikon Digital DS-SMc camera.

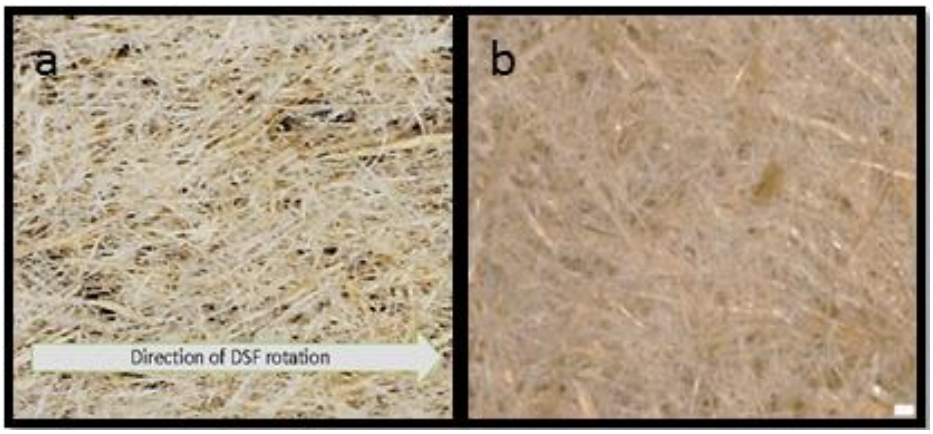

Fig. 5. Macroscopic images of (a) aligned short hemp fibre mat (b) random aligned mat.

2.2.8 Fibre mat production

Aligned fibre mats (Fig. 6a) were produced using a dynamic sheet former (Fig. 6b) built by Canpa, Canada. To produce fibre mats, fibre suspension (approx. 5g in 10 litres of water) was made. This suspension was then pumped by the dynamic sheet former through a reciprocating nozzle onto a rotating drum covered with a wire mesh which acts as a cushion for the deposited fibre (Pickering, Efendy et al. 2015). The alignment of the fibres is in accordance with the nozzle and rotation of the drum. A total of 45g of fibre was used for production of each mat. For the production of fibre mats using DSF, well separated fibre is required to avoid blocks mainly in the flow hoses through which the fibre suspension is discharged onto the rotating drum from the suspension tank.

Randomly aligned fibre mat was also produced by pouring fibre suspension (10g in 10 litres) onto a screen with fine holes through which the water drained. The formed mat was partially drained with paper towels by hand pressing. Finally, both aligned and random mats were oven dried at 80 °C for 48 hours.

Fig. 6. (a) Aligned short hemp fibre mat (b) dynamic sheet former.

2.2.9 Production of composites and testing

A sheet die attached to a ThermoPrism TSE-16-TC twin-screw extruder was used to produce PP/MAPP (100/7.14) sheets. In order to produce composites (except neat PP), the PP/MAPP sheets and the fibre mats were weighed and arranged in stacks between two Teflon sheets before inserting into a mould. The details of the mould used are available in the literature (Pickering and Efendy 2016). The stacking arrangements used for the production of various composites are listed in Table 1. The stacks were heated and pressed in a hot press same as that of neat PP samples (at 170 °C for 5 minutes at 1 MPa). Since the fibre mats are easily distorted, the production process should be carried out carefully. Before the application of pressure, it was ensured that the sheets were fully melted such that the matrix material consolidates sufficiently with the fibre mats. Procedures detailed in ASTM D 638-03; Standard Test Method for Tensile Properties of Plastics was followed for testing the specimens. An Instron-4204 tensile testing machine fitted with a 5 kN load cell, operated at a constant rate of 1mm/min was used for the testing. For the measurement of strain, an Instron 2630-112 extensometer with a gauge length 50 mm was attached to the central part of the test specimen. Before testing, all the samples were conditioned at 23 °C ± 3 °C and

50 % ± 5% relative humidity for at least 48 hours. A total of five samples were tested from each batch.

Table 1: Stacking arrangements used for the production of composites.

Samples		Number of PP* sheets	Number of fibre mats	Fibre wt.% (approx.)	Stack arrangements from bottom to top of the mould
Neat PP		4	0	0	PP/PP/PP/PP
HM-15	P#-HM-15	4	3	15	1PP*/1MAT/1PP*/ 1MAT/1PP*/1MAT/ 1PP*

Note: PP*- PP/MAPP, P#- fibres loaded perpendicular to the DSF rotation direction

3. Results and discussion

3.1 Tensile properties of fibres

Hemp fibres have a complex layered structure, containing primary and secondary cell walls. These cell walls consist of many layers of helically wound cellulose microfibrils. The main factors that determine the mechanical properties of different plant fibres are cellulose content, microfibrillar angle, defects and treatments. (Bledzki and Gassan 1999).

Table 2: Mechanical properties of hemp samples

Hemp Samples	Fibre Diameter (μm)	Maximum Load (N)	Average Tensile Strength (MPa)	Young's Modulus (GPa)
UT	30.25 (10.6)	0.299 (0.14)	517 (355)	7.4 (4.7)
AT/one hour	29.87 (6.7)	0.296 (0.18)	436 (236)	6.4 (2.73)
Granulated before HT	21.38 (4.3)	0.252(0.08)	781 (428)	12.04 (4.4)
Granulated after HT	22.38 (5.8)	0.2784(0.13)	833 (577)	12.32 (7.3)

*Standard deviations are shown in parentheses

Table 2 displays the diameters, maximum load and mechanical properties of untreated and treated fibres obtained in this work. As can be seen, the HT alkali treatment (granulated before and after HT) resulted in more fibre diameter reduction compared to the AT treatment. It has been found that reduction in fibre diameter is due to removal of hemicellulose and lignin (Taha, Steuernagel et al. 2007, John and Anandjiwala 2008, Kabir, Wang et al. 2012, Kabir, Wang et al. 2013). Although no specific studies were carried out to measure the hemicellulose or lignin content in this work, it has been reported elsewhere that hemicellulose breakdown occurs easily in a high

temperature environment than at low temperature and the addition of Na_2SO_3 assists NaOH in the removal of lignin (Beckermann 2007). It was found that HT treatment removed sufficient hemicellulose and lignin from the fibres to give good fibre separation, whereas similar separation was not observed for the fibres with AT treatment.

From the tabulated results, it can be seen that the HT alkali treated fibre exhibited higher average tensile strength and Young's modulus compared to UT and AT alkali treated fibres, whereas the average tensile strength and Young's modulus exhibited by the AT alkali treated fibre were lower than for UT fibre. This suggests that the resulting structures of the treated fibres depend on the alkali treatment used. The increase in average tensile strength for HT alkali treated fibre compared to UT fibre is thought to be due to the removal of weak components (non-strengthening components) evidenced by the fibre diameter reduction after the treatment. The removal of weak components from the fibre cell walls can lead to close packing of cellulose chains and possibly a decrease in the microfibrillar angle. This close compaction could have enhanced the adhesions between cellulose microfibrils, thereby provided better tensile properties for HT treated fibres towards the loading direction compared to UT treated fibres (Efendy and Pickering 2014). As can be seen in Table 2, although the diameter of AT alkali treated fibre reduced after the treatment compared to UT fibre, the tensile properties of the fibre were reduced even below that of UT fibre. The decrease in tensile properties associated with the fibre is thought to be due to the degradation of the crystalline cellulose chains in the microfibrils or bonding between cellulose microfibrils as affected by the AT treatment (Roy, Chakraborty et al. 2012, Efendy and Pickering 2014).

A Student's t-test was carried out for comparing HT alkali treated fibres with different granulation sequence and it was found that the sequence of granulation had no significant effect on tensile properties of the fibres. Weibull modulus, Weibull characteristic strength and experimental average tensile strength are displayed in Table 3. As expected, the characteristic strength has the same trend as that of average tensile strength. The Weibull modulus for the fibres varied from 1.47 to 2.05. These values are comparable with those reported in the literature for cellulosic fibres (Pickering, Beckermann et al. 2007, Ghazali and Efendy 2016).

Table 3: Comparison of Weibull parameters with experimental tensile strength for hemp samples

Hemp Samples	Weibull Modulus, w	Characteristic Strength (MPa), σ_0	Average Tensile Strength (MPa)

UT	1.68	576	517
AT/one hour	1.92	478	436
Granulated before HT	2.05	869	781
Granulated after HT	1.47	928	833

3.2 Crystallinity index (I_c)

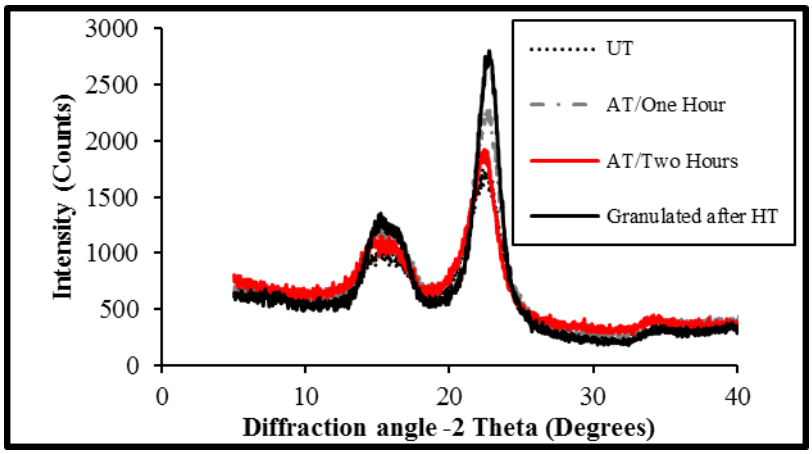

Fig. 7. X-ray diffraction curves for untreated, atmospheric temperature treated and high temperature treated fibres.

Crystallinity index indicates the degree of crystallinity (Mwaikambo and Ansell 2002, Ouajai and Shanks 2005). The X-ray diffraction profiles (curves) of UT, AT/one hour, AT/two hours and granulated after HT treated hemp fibres are shown in Fig. 7. The I_c values were calculated from maximum and minimum intensity crystallographic peaks for each profile which are around $2\theta = 22.7^{o}$ and $2\theta = 18.3^{o}$ respectively and are displayed in Table 4.

Table 4: Crystallinity index for hemp samples

Hemp Samples	Crystallinity Index (I_c)
UT	64.87
AT/ One Hour	71.16
AT/ Two Hours	61.68
Granulated after HT	80.65

As can be seen in Table 4, alkali treatments improved the I_c values except for AT/two hours. The higher I_c value of HT alkali treated fibre compared to the UT fibre would be expected due to the removal of non-crystalline materials and possibly better packing of cellulose chains within the

fibre (Beckermann 2007). Although the I_c value of AT/one hour alkali treated fibres was higher compared to UT fibre, as discussed earlier the tensile strength of this fibre was lower than that of UT fibre. This suggests that chain scission could have overridden the influence of increased crystallinity (Islam, Pickering et al. 2010, Islam, Pickering et al. 2011, Sawpan, Pickering et al. 2011, Ghazali and Efendy 2016). It has been reported elsewhere that the degradation rate of cellulose in alkali is influenced by fibrillar morphology; a more ordered physical structure impedes degradation (Knill and Kennedy 2003). This supports the production of better-packed cellulose chains with HT treatment which would have impeded the diffusion of alkali reducing cellulose degradation compared to AT alkali treated fibres.

3.3 Infrared spectroscopic analysis

Peaks (Fig. 8) in the regions 1730-1740 cm^{-1} and 1200-1300cm^{-1} indicate the hemicellulose and lignin components through the presence of C=O linkages (Abraham, Deepa et al. 2011, Chen, Yu et al. 2011). Peaks at 1737 cm^{-1}, 1252 cm^{-1} and 1201 cm^{-1} for the UT fibres, became smaller for the AT alkali treated fibres and were not visible for HT alkali treated fibres. Reduction of peak heights supports that alkali treatment removed hemicellulose and lignin, with more removal occurring in HT alkali treated fibres compared to AT alkali treated fibres (Olsson and Salmén 2004, Li and Pickering 2008, Peng, Ren et al. 2009, Abraham, Deepa et al. 2011, Islam, Pickering et al. 2011, Kabir, Wang et al. 2013). Similarly, the smaller peaks in the range between 1280 cm^{-1} and 1330 cm^{-1} for HT alkali treated fibre compared to AT alkali treated and UT fibres further support that HT treatment removes more hemicellulose than AT alkali treated fibres (Taha, Steuernagel et al. 2007). The intensity of peaks between 1630 cm^{-1} and 1650 cm^{-1} slightly increased after alkali treatment, which may be due to water molecules formed by the reactions between sodium hydroxide and cellulosic hydroxyl groups (Le Troedec, Sedan et al. 2008).

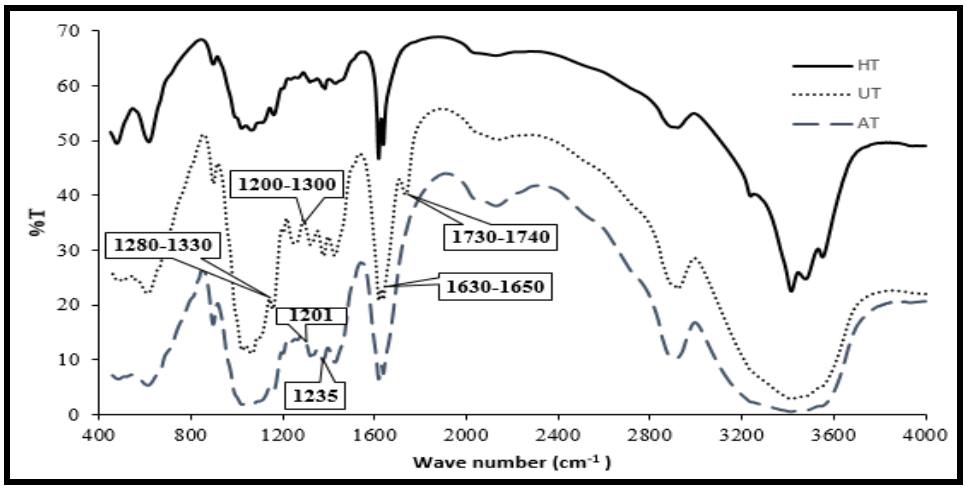

Fig. 8. The FTIR spectra of untreated, AT/one hour treated, and granulated after HT treated fibres.

3.4 Thermal gravimetric analysis (TGA)

Typically, for NPFs, there are three main stages of degradation where most of the weight loss occurs: 50-100 °C due to evaporation of moisture in the fibres, 200-350 °C due to hemicellulose decomposition and 300-500 °C mainly due to degradation of lignin and cellulose (Sun, Tomkinson et al. 2000, Dahiya and Rana 2004, Methacanon, Weerawatsophon et al. 2010).

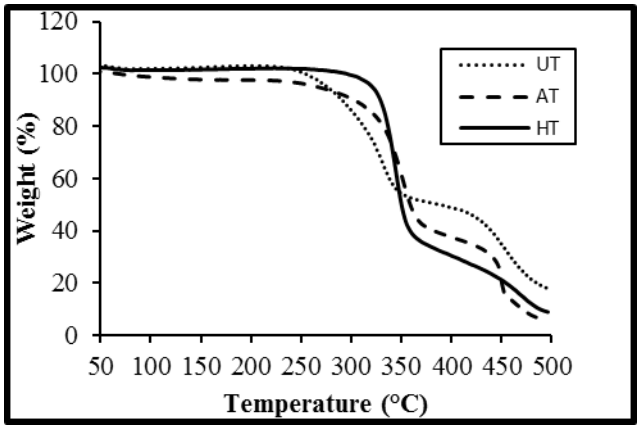

Fig. 9. TGA thermograms for UT, AT/one hour treated, and granulated after HT treated fibres.

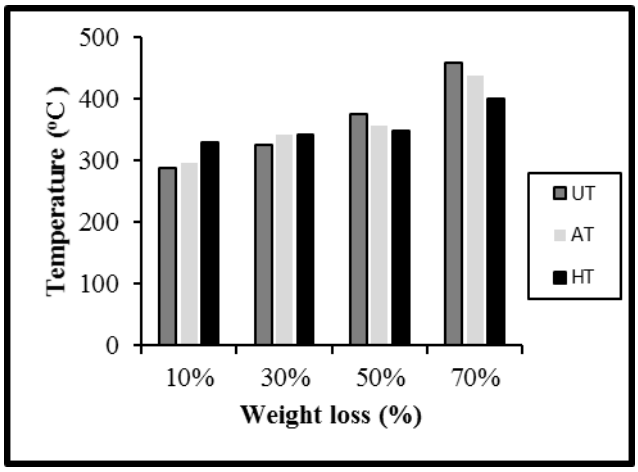

Fig. 10. Weight loss summary for different samples.

Figures 9 and 10 (Fig. 9 and Fig. 10) show the TGA thermograms and weight loss summary for UT fibres, AT and HT alkali treated fibres. From Fig. 10, it can be seen that the initial 10 % weight loss occurred only at 297 °C and 329 °C for the AT and HT alkali treated fibres respectively compared to 288 °C for UT fibres supporting the overall improved thermal stability of the fibres. The improved thermal stability of the fibres is likely to be due to thermally unstable components (hemicellulose and pectin) being removed from the fibres due to alkali treatment (Beckermann 2007), with more removal occurring with HT alkali treatment compared to AT treated fibres as supported by FTIR analysis. As the temperature further increased above 360 °C, the weight loss was lower for UT fibres compared to treated fibres, which may be due to a stable lignocellulose complex formed at higher temperatures that prevented this lignin-rich fibre from further weight loss above 360 °C (Islam 2008). Also, at higher temperatures, it was found that the weight percentage loss was higher for HT alkali treated fibres compared to AT alkali treated fibres (Fig. 10). This higher weight percentage loss for HT alkali treated fibres above 360 °C supports that the greater removal of lignin from the fibre was by HT alkali treatment compared to AT alkali treatment (Beckermann 2007, Ghazali and Efendy 2016). This greater removal was further supported by the higher amount of residue obtained after the TGA analysis for AT treated fibres compared to the HT treated fibres (Beg 2007).

3.5 SEM microscopy of hemp fibre

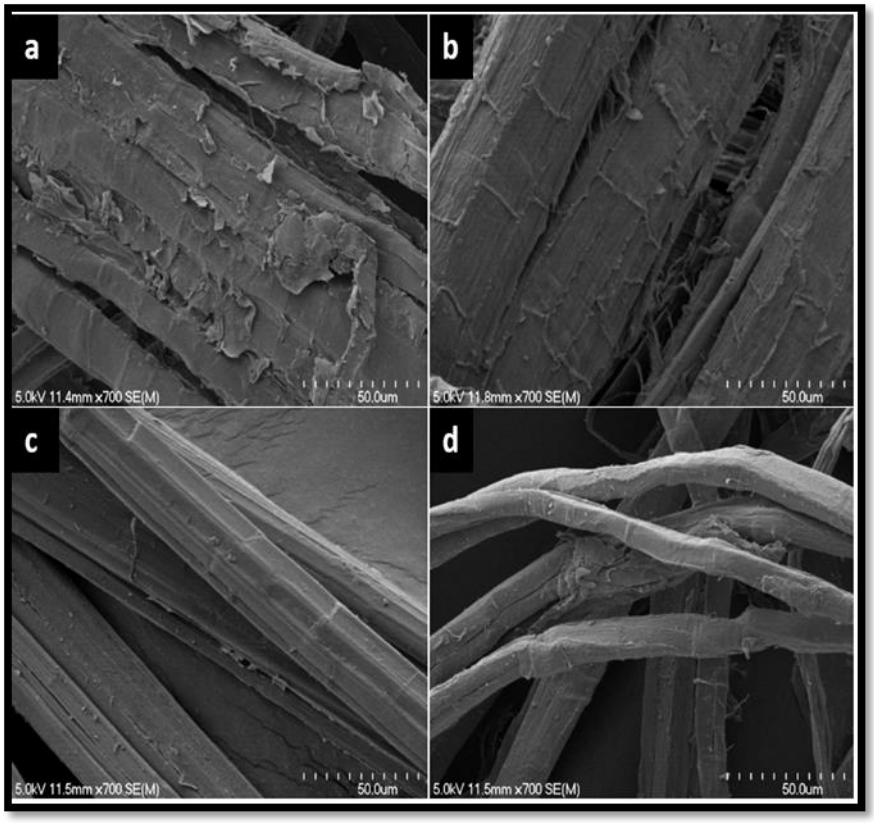

Fig. 11. SEM images of hemp fibre surfaces (a) UT fibre (b) AT/one hour alkali treated fibre (c) granulated before HT alkali treated fibre (d) granulated after HT alkali treated fibre.

Fig. 11 shows the SEM micrographs of hemp fibre. As can be seen in Fig. 11a, the UT fibres are mostly bundle form; substances known to include lignin, pectin, hemicellulose and other non-strengthening components are localised on their surfaces (Ghazali and Efendy 2016). Alkali treated hemp fibres appeared to have undergone some degree of fibre separation known to occur due to the removal of some of these components (Fig. 11b, 11c and 11d). However, it was found that the AT treatment resulted in very little separation of fibres compared to the HT alkali treatment (Fig. 11b). It was also found that the fibres granulated after HT alkali treatment were better separated compared to the fibres granulated before HT alkali treatment, which is evident from Fig. 11d compared to Fig. 11c.

3.6 Fibre mat assessment

It was found that only fibres granulated after HT alkali treatment were sufficiently separated to successfully be used in a dynamic sheet former to form short hemp fibre mats (Fig. 5a and Fig.

6a). Fig. 12 shows the fibre orientation distribution profiles obtained for the mats analysed using OrientationJ (ImageJ). As can be seen for the random mats, there appeared only a relatively small broad peak (almost a flat curve). In contrast, there appeared a sharp predominant peak for the mats produced using DSF around 0 ° (± 5 °), i.e. the preferred orientation direction. The coherency factors generated by the OrientationJ program for the DSF mats and random mats were 0.23 (± 0.028) and 0.11 (0.038), respectively. The predominant peak and higher coherency factor for the DSF mats compared to the broad peak and lower coherency factor for the random mats support the potential of dynamic sheet former to produce aligned short hemp fibre mats.

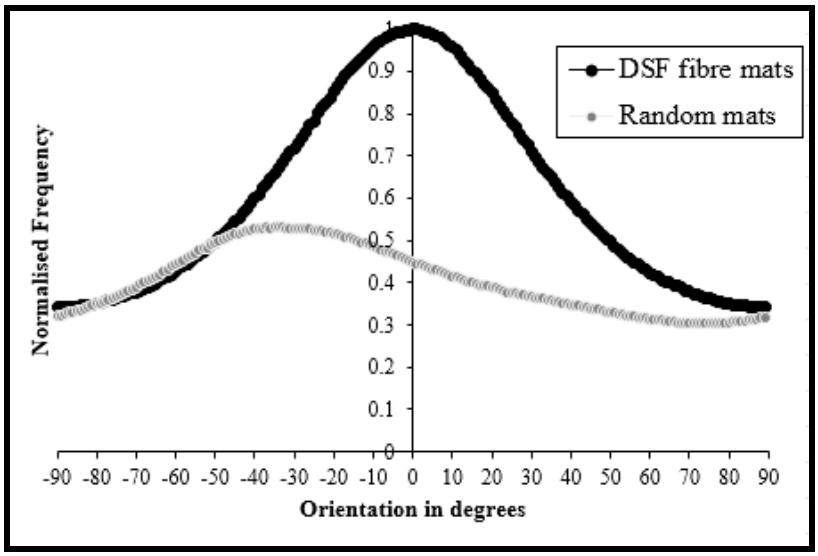

Fig. 12. Fibre orientation distribution profiles obtained by OrientationJ.

3.7 Evaluation of composites

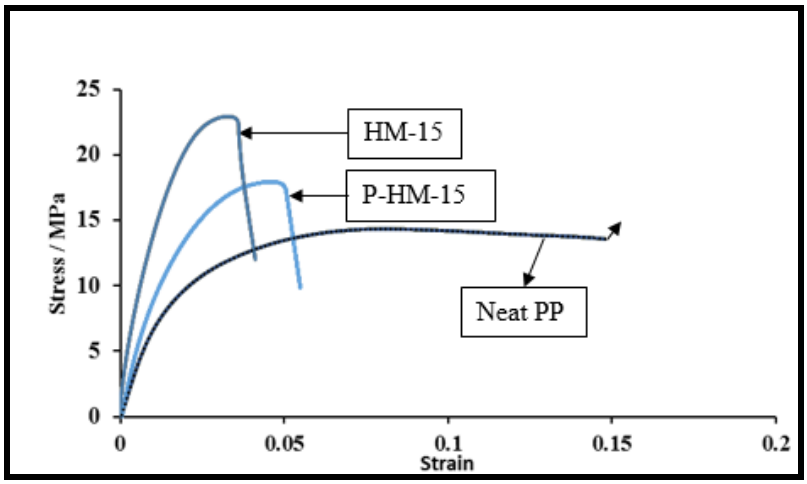

Fig. 13. Typical stress-strain curves for polypropylene reinforced with 15 wt% hemp fibre loaded parallel and perpendicular to the DSF rotation (main fibre orientation) direction.

Composites were tested parallel and perpendicular to the main fibre orientation direction (DSF rotation direction). Fig. 13 shows the stress versus strain curves for the composites with fibre content of 15 wt% along with that of neat PP for comparison purposes. Neat PP extended in a ductile manner to high strain without fail, whereas the incorporation of fibres caused PP to fail in almost a brittle manner without much noticeable yielding.

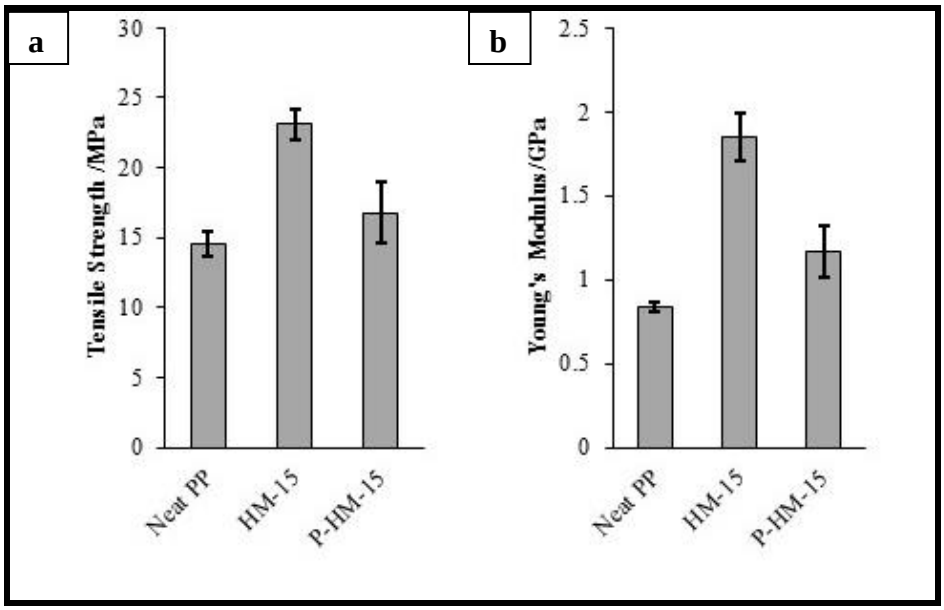

Fig. 14. Graph representing (a) tensile strength and (b) Young's modulus for the hemp composites tested parallel and perpendicular to the DSF rotation direction.

Tensile properties for neat PP along with composites are presented in Fig. 14. The maximum tensile strength and Young's modulus of the composite were approximately 59 and 120 % higher than for neat PP. From the results, it can be seen that composite tested parallel to the main fibre orientation direction exhibited higher tensile properties compared to the composite tested perpendicular to the main fibre orientation direction. This further supports the potential of DSF to produce aligned fibre mats. It has been reported that the best mechanical properties for composites are generally being obtained when the fibres are aligned parallel to the direction of the applied load (Herrera-Franco and Valadez-Gonzalez 2005, Pickering, Efendy et al. 2015).

4. Conclusion

The high temperature treatment at 120 °C using 5wt% NaOH and 2wt% Na_2SO_3, with a fibre to solution ratio of 1:8, improved the tensile strength and Young's modulus of hemp fibres by 51% and 62% respectively compared to untreated fibre. In contrast, tensile strength and Young's

modulus of ambient temperature treated hemp fibre were lower than that of untreated fibres by 16% and 14% respectively. SEM, XRD, FTIR and TGA analyses support that the high temperature treatment removes more non-strengthening components from the fibres compared to ambient temperature treatment. Improvement of fibre strength with high temperature alkali treatment compared with the reduction of fibre strength obtained with ambient temperature alkali treatment suggests better packing of cellulose chains occur for high temperature treatment providing better resistance to cellulose degradation. Therefore, high temperature treatment is recommended for producing strong and stiff fibres for use in natural plant fibre composites. Overall, significantly aligned short hemp fibre mats from high strength hemp fibres was produced using DSF.

Acknowledgements

This research received no specific grant from any agency in the public, commercial, or not-for-profit sectors. However, the authors would like to thank to the University of Waikato's Composites research group for their support.

References

Abraham, E., B. Deepa, L. Pothan, M. Jacob, S. Thomas, U. Cvelbar and R. Anandjiwala (2011). "Extraction of nanocellulose fibrils from lignocellulosic fibres: a novel approach." Carbohydrate Polymers **86**(4): 1468-1475.

Abràmoff, M. D., P. J. Magalhães and S. J. Ram (2004). "Image processing with ImageJ." Biophotonics international **11**(7): 36-42.

ASTM, D. (1986). "3379-75." Standard Test Method for Tensile Strength and Young's Modulus for High-Modulus Single-Filament Materials, Annual Book of ASTM Standards,(May 1989) **8**: 128-131.

Beckermann, G. (2007). "Performance of hemp-fibre reinforced polypropylene composite materials."

Beckermann, G. and K. L. Pickering (2008). "Engineering and evaluation of hemp fibre reinforced polypropylene composites: fibre treatment and matrix modification." Composites Part A: Applied Science and Manufacturing **39**(6): 979-988.

Beg, M. D. H. (2007). The improvement of interfacial bonding, weathering and recycling of wood fibre reinforced polypropylene composites, The University of Waikato.

Biagiotti, J., D. Puglia, L. Torre, J. M. Kenny, A. Arbelaiz, G. Cantero, C. Marieta, R. Llano-Ponte and I. Mondragon (2004). "A systematic investigation on the influence of the chemical treatment of natural fibers on the properties of their polymer matrix composites." Polymer Composites **25**(5): 470-479.

Bledzki, A. and J. Gassan (1999). "Composites reinforced with cellulose based fibres." Progress in polymer science **24**(2): 221-274.

Chen, W., H. Yu, Y. Liu, P. Chen, M. Zhang and Y. Hai (2011). "Individualization of cellulose nanofibers from wood using high-intensity ultrasonication combined with chemical pretreatments." Carbohydrate Polymers **83**(4): 1804-1811.

Dahiya, J. and S. Rana (2004). "Thermal degradation and morphological studies on cotton cellulose modified with various arylphosphorodichloridites." Polymer International **53**(7): 995-1002.

Efendy, M. A. and K. Pickering (2014). "Comparison of harakeke with hemp fibre as a potential reinforcement in composites." Composites Part A: Applied Science and Manufacturing **67**: 259-267.

French, A. D. (2014). "Idealized powder diffraction patterns for cellulose polymorphs." Cellulose **21**(2): 885-896.
Gesellchen, F., A. Bernassau, T. Dejardin, D. Cumming and M. Riehle (2014). "Cell patterning with a heptagon acoustic tweezer–application in neurite guidance." Lab on a Chip **14**(13): 2266-2275.
Ghazali, M. and A. Efendy (2016). Bio-composites materials from engineered natural fibres for structural applications, University of Waikato.
Herrera-Franco, P. and A. Valadez-Gonzalez (2005). "A study of the mechanical properties of short natural-fiber reinforced composites." Composites Part B: Engineering **36**(8): 597-608.
Islam, M., K. Pickering and N. Foreman (2010). "Influence of alkali treatment on the interfacial and physico-mechanical properties of industrial hemp fibre reinforced polylactic acid composites." Composites Part A: Applied Science and Manufacturing **41**(5): 596-603.
Islam, M. S. (2008). The influence of fibre processing and treatments on hemp fibre/epoxy and hemp fibre/PLA composites, the University of Waikato.
Islam, M. S., K. L. Pickering and N. J. Foreman (2011). "Influence of alkali fiber treatment and fiber processing on the mechanical properties of hemp/epoxy composites." Journal of Applied Polymer Science **119**(6): 3696-3707.
John, M. J. and R. D. Anandjiwala (2008). "Recent developments in chemical modification and characterization of natural fiber-reinforced composites." Polymer composites **29**(2): 187-207.
Kabir, M., H. Wang, K. Lau and F. Cardona (2012). "Chemical treatments on plant-based natural fibre reinforced polymer composites: An overview." Composites Part B: Engineering **43**(7): 2883-2892.
Kabir, M., H. Wang, K. Lau and F. Cardona (2013). "Effects of chemical treatments on hemp fibre structure." Applied Surface Science **276**: 13-23.
Kabir, M., H. Wang, K. Lau and F. Cardona (2013). "Tensile properties of chemically treated hemp fibres as reinforcement for composites." Composites Part B: Engineering **53**: 362-368.
Kabir, M., H. Wang, K. Lau, F. Cardona and T. Aravinthan (2012). "Mechanical properties of chemically-treated hemp fibre reinforced sandwich composites." Composites Part B: Engineering **43**(2): 159-169.
Knill, C. J. and J. F. Kennedy (2003). "Degradation of cellulose under alkaline conditions." Carbohydrate Polymers **51**(3): 281-300.
Le, T. M. (2016). Harakeke fibre as reinforcement in epoxy matrix composites and its hybridisation with hemp fibre, University of Waikato.
Le, T. M. and K. L. Pickering (2015). "The potential of harakeke fibre as reinforcement in polymer matrix composites including modelling of long harakeke fibre composite strength." Composites Part A: Applied Science and Manufacturing **76**: 44-53.
Le Troedec, M., D. Sedan, C. Peyratout, J. P. Bonnet, A. Smith, R. Guinebretiere, V. Gloaguen and P. Krausz (2008). "Influence of various chemical treatments on the composition and structure of hemp fibres." Composites Part A: Applied Science and Manufacturing **39**(3): 514-522.
Lewis, D. D. J. (2016). Interlaminar reinforcement of carbon fiber composites from unidirectional prepreg utilizing aligned carbon nanotubes, Massachusetts Institute of Technology.
Li, X., L. G. Tabil and S. Panigrahi (2007). "Chemical treatments of natural fiber for use in natural fiber-reinforced composites: a review." Journal of Polymers and the Environment **15**(1): 25-33.
Li, Y. and K. L. Pickering (2008). "Hemp fibre reinforced composites using chelator and enzyme treatments." Composites Science and Technology **68**(15): 3293-3298.
Methacanon, P., U. Weerawatsophon, N. Sumransin, C. Prahsarn and D. Bergado (2010). "Properties and potential application of the selected natural fibers as limited life geotextiles." Carbohydrate Polymers **82**(4): 1090-1096.
Mwaikambo, L. Y. and M. P. Ansell (2002). "Chemical modification of hemp, sisal, jute, and kapok fibers by alkalization." Journal of applied polymer science **84**(12): 2222-2234.
Olsson, A.-M. and L. Salmén (2004). "The association of water to cellulose and hemicellulose in paper examined by FTIR spectroscopy." Carbohydrate research **339**(4): 813-818.
Ouajai, S. and R. Shanks (2005). "Composition, structure and thermal degradation of hemp cellulose after chemical treatments." Polymer degradation and stability **89**(2): 327-335.
Oushabi, A., S. Sair, F. O. Hassani, Y. Abboud, O. Tanane and A. El Bouari (2017). "The effect of alkali treatment on mechanical, morphological and thermal properties of date palm fibers (DPFs): Study of the interface of DPF–Polyurethane composite." South African Journal of Chemical Engineering **23**: 116-123.
Palmieri, V., D. Lucchetti, A. Maiorana, M. Papi, G. Maulucci, F. Calapà, G. Ciasca, R. Giordano, A. Sgambato and M. De Spirito (2015). "Mechanical and structural comparison between primary tumor and lymph node metastasis cells in colorectal cancer." Soft matter **11**(28): 5719-5726.

Peng, F., J.-L. Ren, F. Xu, J. Bian, P. Peng and R.-C. Sun (2009). "Comparative study of hemicelluloses obtained by graded ethanol precipitation from sugarcane bagasse." Journal of agricultural and food chemistry **57**(14): 6305-6317.
Pickering, K. (2008). Properties and performance of natural-fibre composites, Elsevier.
Pickering, K., G. Beckermann, S. Alam and N. Foreman (2007). "Optimising industrial hemp fibre for composites." Composites Part A: Applied Science and Manufacturing **38**(2): 461-468.
Pickering, K. and M. A. Efendy (2016). "Preparation and mechanical properties of novel bio-composite made of dynamically sheet formed discontinuous harakeke and hemp fibre mat reinforced PLA composites for structural applications." Industrial Crops and Products **84**: 139-150.
Pickering, K., M. A. Efendy and T. Le (2015). "A review of recent developments in natural fibre composites and their mechanical performance." Composites Part A: Applied Science and Manufacturing.
Pickering, K. and T. M. Le (2016). "High performance aligned short natural fibre–Epoxy composites." Composites Part B: Engineering **85**: 123-129.
Püspöki, Z., M. Storath, D. Sage and M. Unser (2016). Transforms and operators for directional bioimage analysis: a survey. Focus on Bio-Image Informatics, Springer**:** 69-93.
Rezakhaniha, R., A. Agianniotis, J. T. C. Schrauwen, A. Griffa, D. Sage, C. v. Bouten, F. Van de Vosse, M. Unser and N. Stergiopulos (2012). "Experimental investigation of collagen waviness and orientation in the arterial adventitia using confocal laser scanning microscopy." Biomechanics and modeling in mechanobiology **11**(3-4): 461-473.
Roy, A., S. Chakraborty, S. P. Kundu, R. K. Basak, S. B. Majumder and B. Adhikari (2012). "Improvement in mechanical properties of jute fibres through mild alkali treatment as demonstrated by utilisation of the Weibull distribution model." Bioresource technology **107**: 222-228.
Sawpan, M. A., K. L. Pickering and A. Fernyhough (2011). "Effect of various chemical treatments on the fibre structure and tensile properties of industrial hemp fibres." Composites Part A: Applied Science and Manufacturing **42**(8): 888-895.
Schneider, C. A., W. S. Rasband and K. W. Eliceiri (2012). "NIH Image to ImageJ: 25 years of image analysis." Nature methods **9**(7): 671-675.
Segal, L., J. Creely, A. Martin Jr and C. Conrad (1959). "An empirical method for estimating the degree of crystallinity of native cellulose using the X-ray diffractometer." Textile research journal **29**(10): 786-794.
Shah, D. U., F. Vollrath, J. Stires and D. D. Deheyn (2015). "The biocomposite tube of a chaetopterid marine worm constructed with highly-controlled orientation of nanofilaments." Materials Science and Engineering: C **48**: 408-415.
Sun, R., J. Tomkinson and G. L. Jones (2000). "Fractional characterization of ash-AQ lignin by successive extraction with organic solvents from oil palm EFB fibre." Polymer Degradation and Stability **68**(1): 111-119.
Sunny, T., K. L. Pickering and S. H. Lim (2017). Alignment of Short Fibres: An Overview. Processing and Fabrication of Advanced Materials-XXV.
Sunny, T., K. L. Pickering and S. H. Lim (2018). Fibre Orientation Distribution Assessment of Dynamically Sheet Formed Hemp Fibre Mats by Image Analysis. Applied Mechanics and Materials, Trans Tech Publ.
Taha, I., L. Steuernagel and G. Ziegmann (2007). "Optimization of the alkali treatment process of date palm fibres for polymeric composites." Composite Interfaces **14**(7-9): 669-684.
Zafeiropoulos, N. and C. Baillie (2007). "A study of the effect of surface treatments on the tensile strength of flax fibres: Part II. Application of Weibull statistics." Composites Part A: Applied Science and Manufacturing **38**(2): 629-638.